



Fermi National Accelerator Laboratory

FERMILAB-FN-583

## Calorimetry and Radiation Damage

Dan Green

*Fermi National Accelerator Laboratory  
P.O. Box 500, Batavia, Illinois 60510*

June 1992

Invited talk given at the *International Conference on Radiation-Tolerant Scintillators and Detectors*,  
April 28 - May 2, 1992, Florida State University, Tallahassee, Florida



## **Disclaimer**

*This report was prepared as an account of work sponsored by an agency of the United States Government. Neither the United States Government nor any agency thereof, nor any of their employees, makes any warranty, express or implied, or assumes any legal liability or responsibility for the accuracy, completeness, or usefulness of any information, apparatus, product, or process disclosed, or represents that its use would not infringe privately owned rights. Reference herein to any specific commercial product, process, or service by trade name, trademark, manufacturer, or otherwise, does not necessarily constitute or imply its endorsement, recommendation, or favoring by the United States Government or any agency thereof. The views and opinions of authors expressed herein do not necessarily state or reflect those of the United States Government or any agency thereof.*

# CALORIMETRY AND RADIATION DAMAGE

Dan Green

Fermi National Accelerator Laboratory  
Batavia, IL 60510

## ABSTRACT

The rationale for scintillator based calorimetry at the SSC and its operation are briefly discussed. The SSC radiation dose and its effect on calorimeter operation are examined. Data from  $\text{Co}^{60}$  and e beam tests are used to set the scale of these effects.

## INTRODUCTION

The goal of the next generation of collider detectors is to study the origin of electroweak symmetry breaking. The mass scale for this study has an upper bound of about 1 TeV. At that mass, weak interactions become strong in that they violate partial wave unitarity (Eichten *et al.*, 1984). The S wave amplitude,  $\alpha_o$ , for  $ee \rightarrow WW$  scattering is;

$$\begin{aligned} \alpha_o &\sim \alpha_W / 4\pi(M / M_W)^2, \alpha_W \sim 1/30 \\ &\sim 1 \text{ if } M \sim 1.6 \text{ TeV} \end{aligned} \quad (1)$$

One is then guaranteed that new phenomena occur at or below this mass. Detectors for the SSC must therefore confront this mass scale. The effects of electroweak symmetry breaking (Higgs) are expected to be large in 2 gauge boson final states. Given that the simplest decay modes (experimentally) of gauge bosons are into leptons, there is a premium at the SSC on final state lepton detection (Green, 1991a).

Unfortunately, the Higgs coupling to ordinary matter is rather weak. This means that the study of multiple gauge boson final states at high mass is rate limited due to the low production cross section. Therefore, the luminosity of the SSC has been designed to be 1000 times the design luminosity of the FNAL collider. The combination of high mass scales, and thus high energies, and weak coupling, and thus high machine luminosity, means that SSC detectors are naturally concerned with radiation damage. The SSC rf bunch separation of 16 nsec means that fast detectors are at a premium. Slow detectors would sum over many interactions, thus confusing the kinematics of the individual interactions. Hence, this Conference on radiation tolerant scintillators.

## WHY SCINTILLATOR CALORIMETRY?

Calorimetry will be the cornerstone of the new SSC detectors. First, it plays a role in identifying and/or measuring ALL the components of the Standard Model. In particular, leptons appear as missing energy, or electromagnetic (EM) showers, or minimum ionizing towers, or narrow jets for neutrinos, electrons, muons, or taus respectively. The calorimeter measures the magnitude, position, and time of energy deposition over some angular range.

In addition, calorimetry is the technology whose fractional energy resolution actually improves with energy (or at worst remains constant). By contrast, the fractional error in tracking detectors becomes linearly worse with the energy. Finally, the depth needed to contain a particle within the calorimetry increases only logarithmically with the incident particle energy. Thus, SSC calorimeters are still relatively compact (Green *et al.*, 1991b).

The event rates at the SSC are of order 100 MHz. The detection processes in calorimeters are intrinsically fast- of order 25 nsec (Cushman, 1991). Therefore, it is natural to concentrate on scintillation based calorimetry at the SSC since it does not degrade the speed of calorimetric detection processes. Many studies have been done on the Physics processes of interest at the SSC and the requirements which they imply for SSC calorimetry (Siegrist, 1991). The performance of a typical calorimeter with respect to those requirements has also been documented (SDC, 1991). The layout of a "typical" SSC experiment, the SDC detector, is shown in Fig. 1. The people shown set the scale of the detector. Note that, even though the energy is 20 times that of the FNAL collider, the size of the calorimeter itself has only grown modestly with respect to those of CDF and DØ.

## CALORIMETER OPERATION

Calorimetry is explained in many review articles (Cushman, 1991). For our purposes, it is sufficient to make a grossly simplified model of a calorimeter. The incident particle, of energy  $E_0$ , develops a "shower" through successive interactions. Every distance  $X_0$  another interaction with mean multiplicity  $n$  occurs, and the final state products share the energy equally. Therefore at a depth of  $pX_0$  the shower contains  $n^p = N$  particles, each of energy  $E_0/N$ . The shower continues to grow until new particles cannot be made, at a particle energy of  $E_c$ . After this "shower max" point is reached, the shower dies off rapidly as the shower particles lose energy by ionization. The maximum number of particles (shower max) is then  $N_{max} = E_0/E_c$ . Shower max occurs at a depth  $pX_0$  where  $n^p = N_{max}$ . Just to set a physical scale,  $X_0$  for EM showers in Pb is 0.56 cm, and  $E_c$  is 8.7 MeV. The corresponding length for hadronic showers is 16.76 cm in Fe and the threshold for pion production is  $E_c \sim 320$  MeV.

A variety of conclusions follow from this toy model. The calorimeter is linear; a measure of  $N_{max}$  is proportional to  $E_0$ . One expects that statistical fluctuations in  $N_{max}$  lead to energy errors,  $dE/E \sim \sqrt{1/N_{max}} \sim b/\sqrt{E}$ . Therefore, fractional calorimeter energy measurements improve with energy. Finally the containment depth,  $X_{max} = pX_0$  is logarithmically related to the incident energy,  $p \log(n) = \log(E_0/E_c)$ .

$$\begin{aligned}
E &= a E_0 \\
dE / E &= b / \sqrt{E} \\
X_{\max} &= c \ln (E_0 / Ec)
\end{aligned}
\tag{2}$$

A fit to a real Monte Carlo simulation of EM showers yields a parametrization for the deposited energy  $dE$  in thickness  $dt = d(z/X_0)$ :

$$\begin{aligned}
dE(u) / E_0 &= u^{a-1} e^{-u} du / \Gamma(a) \\
u &= bt, \quad b \sim 0.5 \\
a &= 1 + b[\ln(E_0 / Ec) + c]
\end{aligned}
\tag{3}$$

Note the rapid rise to shower max implied by the  $u^{a-1}$  factor followed by the falloff given by the  $\exp(-u)$  factor. The location of shower max is logarithmically related to the incident energy,  $E_0$ . For an energy of 100 GeV, shower max is at  $\sim 9 X_0$ .

### RADIATION DOSE

The dose,  $D$ , can also be understood simply. Inelastic interactions at the SSC occur with a particle rate which is uniform in azimuth and rapidity,  $dN \sim dyd\phi$ . These particles may be thought to have a fixed momentum,  $P_t$ , transverse to the incident beams. Thus, the energy deposited by the reaction products goes as,  $dE \sim [P_t / \sin \theta] dyd\phi$ . For small angles,  $dy = d\theta / \theta$ . Therefore, for a detector element of area  $dA$  at radius  $R$ , the energy deposit, and hence the dose times weight, is proportional, at small angles, to

$$\begin{aligned}
dE &\sim D dA dz \rho \\
&\sim [P_t / \theta^3] [dA / R^2]
\end{aligned}
\tag{4}$$

where  $\rho$  is the density of the detector.

The energy deposited by these particles is spread throughout the calorimeter. The most localized region occurs at EM shower maximum. Hence, the worst case for a given angle appears at the EM shower max depth. The dose at shower max is expected to have a  $1/\theta^3$  dependence. A plot of the EM maximum dose as a function of angle for the SDC geometry is shown in Fig.2. Note that over much of the angular range the dose for 100 years of operation at SSC design luminosity is  $< 1$  Mrad. However, in the forward region the steep angular dependence means that the dose rises to  $\sim 60$  Mrad at 5.7 degrees.

### UNIFORMITY AND LINEARITY

The considerations above imply that calorimeters which are uniformly constructed will respond linearly with a fractional error,  $dE/E$  which continues to improve as  $E$  increases. Obviously, there is a limit to this scaling,  $dE / E = b / \sqrt{E}$ . That limit is reached when the nonuniformity of the medium (Pb and scintillator) becomes a factor. In Fig. 3 is shown the tile/fiber layout for the SDC baseline design, the "sigma" tile. The transverse response map

for that tile is also shown in Fig. 2, and has a rms deviation of 2.2%. Monte Carlo methods have been used (SDC, 1991) to relate the nonuniformity to the induced energy error which arises when the transversely nonuniform medium is integrated over. An error in the scintillator light yield of 4% causes a 1% energy error  $dE/E$ , for example. Therefore, a 2% plate to plate or tile to tile thickness nonuniformity will cause a minimum energy error of  $\sim 0.5\%$ .

A similiar study of hadronic shower response was made but real data was used. The conclusion was similar to that for EM showers. The induced "constant term" in the fractional energy resolution is linear in the rms error and energy independent. The slope for hadronic showers is slightly steeper; a 5% rms error causes a 2% error,  $dE/E$ .

$$\frac{dE}{E} = \sqrt{(b/\sqrt{E})^2 + a^2} \quad (5)$$

Therefore, all "real" calorimeters have a minimum resolution which appears at high energies, the "constant term". The value of that minimum depends on the care with which the calorimeter has been constructed. Transverse uniformity is important since particles illuminate all impact points of the calorimeter. Longitudinal uniformity is important because of fluctuations in the way the shower develops. For example, a EM (hadronic) shower has a spread in depth of  $\pm X_0 = 0.56$  cm (16.76 cm) due to fluctuations in the depth at which a photon (hadron) shower starts. If the medium is nonuniform, the resolution will be compromised by these, and other, fluctuations.

## EFFECTS OF RADIATION DAMAGE

Radiation damage for scintillator based calorimetry is in the optical domain. For example, the mean transverse momentum of neutral pions at the SSC is approximately,  $P_t \sim 0.6$  GeV. At the smallest angles covered by SDC with tile/fiber scintillator, the energy is  $E \sim 6$  GeV. The photons will shower in the EM Pb part of the calorimetry, as described by Eq. 3 above. The energy deposited by the shower will damage the optical properties of the scintillator. Aside from an overall light output loss, the shape of Eq. 3 implies that the calorimeter has become a nonuniform medium. Therefore, it will no longer respond linearly and it will have a minimum achievable value of the energy resolution which degrades with increasing dose  $D$ .

If it is assumed that the reduced response is proportional to the local energy deposited by EM showers, then the normalized calorimeter response function,  $WT(z)$ , as a function of depth  $z$ , would become;

$$\begin{aligned} WT(z) &= 1 - d(z) \\ d(z) &= g dE(z), \text{ for } P_t = 0.6 \text{ GeV} \end{aligned} \quad (6)$$

where  $d(z)$  is the "damage profile" which is assumed to be proportional to the energy deposition profile of the inelastically produced neutral pions.

The possible effects of radiation damage on transverse uniformity are not so clear. Since the radiation is thought to produce color centers that reduce the optical attenuation length preferentially at short wavelengths, the tile/fiber wavelength shifting scheme would appear

to be vulnerable. A layout as in Fig. 2 which is optimized for undamaged plastic could conceivably suffer large transverse nonuniformities in the presence of radiation damage.

In order to test the viability of SDC designs, several test modules of depth  $20 X_0$  were built and sent to e test beams. These modules were meant to have identical optics to the candidate calorimeters. They also had Am sources fixed to the PMT which were used to supply an absolute calibration point. In addition, they were outfitted with thin hollow steel tubes deployed both longitudinally and transversely which crossed the center of the tiles in the case of transverse motion. The routing of these tubes allowed a moving Cs source to be used to monitor and measure the damage profile in both directions (Barnes *et al.*, 1990). The e beams were in the range 1.3 to 5.0 GeV which is appropriate to the typical secondary particles produced at the SSC, i.e.  $P_t \sim 0.6$  GeV,  $\theta > 6$  degrees.

### EM STUDIES IN e BEAMS AT ORSAY, KEK, AND BEIJING

Data was taken by groups from Saclay (Bonamy *et al.*, 1991), Tsukuba (Funaki *et al.*, 1991) and IHEP, FNAL (Hu *et al.*, 1991). The data are consistent which gives some confidence in the conclusions. The fact that identical modules were used served to reduce the effects of random variables which have made test results difficult to interpret in the past. It was also crucial to crosscheck the results obtained with e beams against those found using Co exposures. Beam time with e beams is often hard to obtain. Therefore, if Co results could be shown to reproduce the effects of e beam exposures, the range of measurements could be greatly extended.

Data from Co exposures at Tsukuba are shown in Fig. 4. The Co exposure was nonuniform, and the before and after transverse map shows that (at 0.62 Mrad) the optical system has not suffered an induced transverse nonuniformity.

Results from Beijing are shown in Fig. 5 for a typical unexposed longitudinal module source scan. The 20 peaks due to passage by the 20 tiles in depth are clearly seen. Source scans, both transverse and longitudinal, were made during exposures and during post exposure annealing studies. The Beijing modules were exposed in air or N<sub>2</sub> and annealed in air or N<sub>2</sub>. After 60 days post exposure, all modules had the same response profile  $WT(z)$  for a 6 Mrad exposure. Note that the dose rates were high in all cases,  $> 1$  Mrad/day. Figure 6 shows the transverse and longitudinal scans of a module exposed to 1 Mrad of 1.3 GeV electrons. The module face was swept uniformly across the e beam, insuring a uniform transverse dose. As with the Tsukuba data, the transverse source scan at shower maximum indicates that the induced transverse nonuniformity is small.

Two methods of normalization were tried. First, the Am source was used as an absolute scale (assuming the source scintillator, which was placed on the PMT face, and was Pb shielded, was undamaged). Second, the scans were fixed to  $WT = 1$  at tile 20, where the damage was thought to be minimal. Both methods agreed within errors. Fig. 6 shows the profile  $WT(z)$  for a 1.0 Mrad exposure and up to 7.5 days annealing in air. The profile is consistent with the hypothesis of local damage as stated in Eq.6. Note that there is some tile to tile crosstalk in the Cs source scans which has not yet been deconvoluted.

Data from Saclay yields detailed exposures up to 2 Mrad. The Tsukuba data went up to 4 Mrad, while the Beijing data went to 6 Mrad. A compilation of all the data is shown in Fig. 7. The data for  $WT(z)$  at shower max is plotted as a function of dose,  $D$ . Very roughly, the response is related to the dose as,

$$[WT(z)]_{min} \sim \exp(-D/D_0) \quad (7)$$

where the characteristic dose,  $D_0$ , for SCSN81/BCF91 is  $\sim 3.6$  Mrad. At the level of 10% in  $[WT(z)]_{min}$  the data for the 3 experiments do not agree. Given the slight beam and dosimetry differences, this spread can be taken as the systematic error associated with the experiments. Both the Tsukuba and Beijing data indicate a faster than exponential drop at low,  $< 2$  Mrad, doses. At doses  $> 2$  Mrad the exponential behavior represents the data fairly well.

## DOSE/DAMAGE AND ENERGY RESOLUTION

What is the effect of the induced longitudinal nonuniformity on the response of a EM calorimeter? Insights may be obtained by fluctuating a shower of shape given by Eq. 3 in its point of conversion by a standard deviation. That means pick  $t = 1 \pm 1$  where  $t$  is the conversion point in  $X_0$  units. By fluctuating a fixed shower shape on a damaged calorimeter characterized by Eq. 6 and studying the total response  $E$  with respect to the incident energy  $E_0$  (Green *et al.*, 1991c), one can estimate the effects of radiation damage.

Monte Carlo analysis has also been used (Funaki *et al.*, (1991), (Green *et al.*, 1991c). A plot from Ref. 9, given in Fig. 8, shows the fractional induced energy error as a function of peak damage  $[d(z)]_{max}$ . The data shows some modest energy dependence, with higher energies suffering less induced error. This is to be expected, as it was argued in Eq. 2 and Eq. 3 that the damage is caused by showers of energy  $< 6$  GeV while higher energy showers peak deeper. Thus higher energy showers deposit the bulk of their energy in undamaged regions. The induced error is roughly energy independent and linear in the peak damage,

$$(dE / E)_{rad} \sim 0.06 [d(z)]_{max} \quad (8)$$

Therefore, for low energy electrons, if one wants to do calorimetry to an ultimate precision of 1.0%, the peak damage must be kept to  $\sim 16\%$ , or dose to 0.6 Mrad. A glance at Fig.2 shows that this condition is barely met in the SDC barrel.

In Fig. 9 is shown the induced fractional energy error as a function of energy for peak damages of  $[d(z)]_{max} = 0.1, 0.3, \text{ and } 0.5$  (Green *et al.*, 1991c). Also plotted as the shaded area, is the resolution of a rather good EM calorimeter with a statistical or "stochastic" term, Eq. 2, of  $10\% / \sqrt{E}$  and a "constant" term, due to nonuniformities in construction of 0.5% added in quadrature. Note that the induced error decreases as the log of the energy, as expected, and that it is roughly linear in the peak damage. Note also that the effect of radiation damage nowhere exceeds the intrinsic errors of the EM calorimeter if  $[d(z)]_{max} < 0.3$ .

The reason for the reduced sensitivity to peak damage with respect to Fig. 8 is that in Fig. 9 it was assumed that the EM calorimeter has 2 independent energy measurements in depth. These 2 measurements allow one to estimate the photon conversion point. Thus, knowing the response profile  $WT(z)$  (using source tubes) one can correct for some of the fluctuations in the EM shower development. This technique at least halves the coefficient given in Eq. 8 and has lead SDC to require physical segmentation of all EM calorimetry.

damaged region, a larger fraction of their signal reaches the output. Therefore, the radiation damage which generates a nonuniform medium makes for a nonlinear energy response. Details may be found in Ref. 11. Suffice it to say that for  $[d(z)]_{max} < 0.3$ , knowing  $WT(z)$  and using 2 longitudinal "compartments", one can correct such that the induced residual nonlinearity is everywhere less than the intrinsic energy error assuming a 10% "stochastic" and a 0.5% "constant" term.

## HADRONIC SIMULATIONS

Hadronic showers are rather more complex than EM showers. Therefore, one tends to use data to simulate radiation damage. As argued above, the EM calorimeters have the largest dose since the EM showers have the shortest characteristic length,  $X_0$ , and thus the highest energy density. However, the steep angular dependence, Eq. 4, of the dose means that the endcap hadronic region also suffers doses  $> 1$  Mrad. In Fig. 10 is shown a simulated damage profile for hadrons. It is assumed that the damage mirrors the local energy deposition as in Eq. 6. Data in a HAD calorimeter with 15 GeV incident hadrons are used to simulate the low energy inelastic reaction products. The coefficient of  $dE(z)$  for the hadron showers was adjusted in Fig. 10 to give a peak damage of 20%. Note that the damage spreads over the entire 10 nuclear absorption length depth of SDC hadronic calorimetry.

Using the simulated damage profile given in Fig. 10, one weighs the individually read out layers of the calorimeter and looks at the induced nonlinearity and fractional energy resolution for an ensemble of hadrons at different energies. Again data were used rather than using Monte Carlo methods. This strategy was adopted because the hadronic showers have large fluctuations which are hard to model.

Both effects appear to be roughly energy independent and linear in the peak damage, as plotted in Fig. 11.

$$\begin{aligned} (dE / E)_{rad} &\sim 0.25 [d(z)]_{max} \\ [ \langle E(d) \rangle - \langle E(0) \rangle ] / \langle E(0) \rangle &\sim 0.70 [d(z)]_{max} \end{aligned} \quad (9)$$

The sensitivity of the hadronic calorimeter measurements to radiation damage is about four times greater than the EM sensitivity. This fact is due to the larger fluctuations inherent in hadron showers which lead to a rather unlocalized response profile,  $WT(z)$ , and to hadronic showers that populate a large and fluctuating fraction of the calorimeter.

## SUMMARY AND FUTURE DIRECTIONS

The current work has established an existence proof for SDC barrel calorimetry. In the forward or endcap region doses 100 times larger will be suffered, and one must, at present, contemplate replacement of the scintillator every few years for operation at SSC design luminosity. One possible avenue is to monitor and measure the damage. Source tubes will allow for a continuous measurement of  $WT(z)$ . In situ calibration using  $e$  from  $Z \rightarrow ee$  decays can be used to track the calibration. Finally, longitudinal segmentation will be used to reduce the sensitivity of isolated  $e$  to shower conversion point fluctuations. All these methods will allow SDC to operate with a reduced sensitivity as shown in Fig. 9.

To go beyond this point with existing plastics one needs to bias the optics to longer wavelengths. The color center model for radiation damage, and the measurements of the wavelength dependence of damage (Bross *et al.*, 1989) point toward tile operation in the green. An initial attempt at this operation using SCSN81+Y7/O2 was not successful and in addition had a light loss of 3x using standard green extended PMT (Byon-Wagner). Red sensitive PMT are needed if one is to operate with sufficient photostatistics. We must understand why the first attempt to go from blue/green to green/orange failed. Fiber damage appears to be one factor (Foster).

Finally, we await miracles from the chemists. New plastics are the Godot for whom we wait. We promise fast evaluation of any candidate scintillator which appears.

## REFERENCES

- Barnes, V. and A. Laasanen (1990). Symposium on Detector Research and Development for the SSC.
- Beretvas, A., D. Green, J. Marraffino and W. Wu (1992). Hadronic Energy Resolution and Radiation Damage, Fermilab-FN-582.
- Bonamy, P., G. Dubost, J. Ernwein, R. Hubbard, P. Le Du, F. Rondeaux and G. Villet (1991). Radiation Damage in Tile-Fiber Calorimeter Modules, SDC-91-126.
- Bross, A. and A. Pla-Dalmau (1990). Proceedings of the First International Conference on Calorimetry in High Energy Physics, World Scientific.
- Byon-Wagner, A. Private Communication.
- Cushman, P. (1991). Electromagnetic and Hadronic Calorimeters, YCTP-P47-91.
- Eichten, E. *et al.*, (1984). *Rev. Mod. Phys.* 56 4, 579.
- Foster, G.W. Private Communication.
- Funaki, S. *et al.* (1991). Beam Test on Radiation Hardness of a Scintillating Tile/Fiber Calorimeter, SDC-91-85.
- Green, D. (1991a). Physics Requirements for LHC/SSC Calorimetry, FNAL-Conf-91/281.
- Green, D., A. Beretvas, K. Denisenko, N. Denisenko, J. Marraffino, A. Para and W. Wu (1991b). Depth Requirements in SSC Calorimeters, Fermilab-FN-570.
- Green, D., A. Para and J. Hauptman (1991c). Radiation Damage, Calibration and Depth Segmentation in Calorimeters, Fermilab-FN-565.
- Hu, L. *et al.* (1991). Radiation Damage of Tile/Fiber Scintillator Modules for the SDC Calorimeter, SDC-91-119.
- SDC (1991). Calorimeter Conceptual Design Report.
- Siegrist, J., Ed. (1991). SDC Calorimeter Design Requirements.

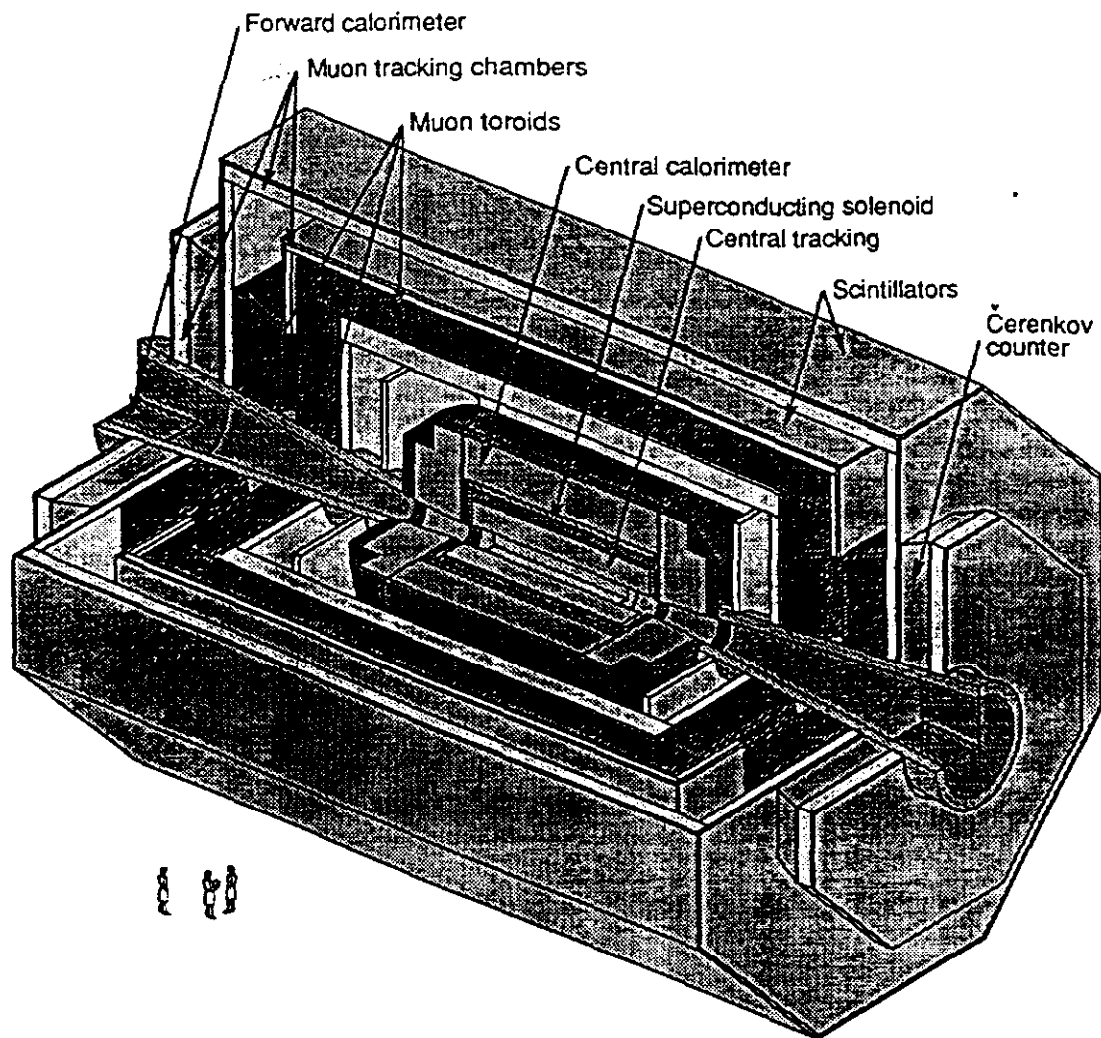


Fig. 1. The SDC detector. The calorimetry is exterior to the magnetic volume provided by the solenoid.

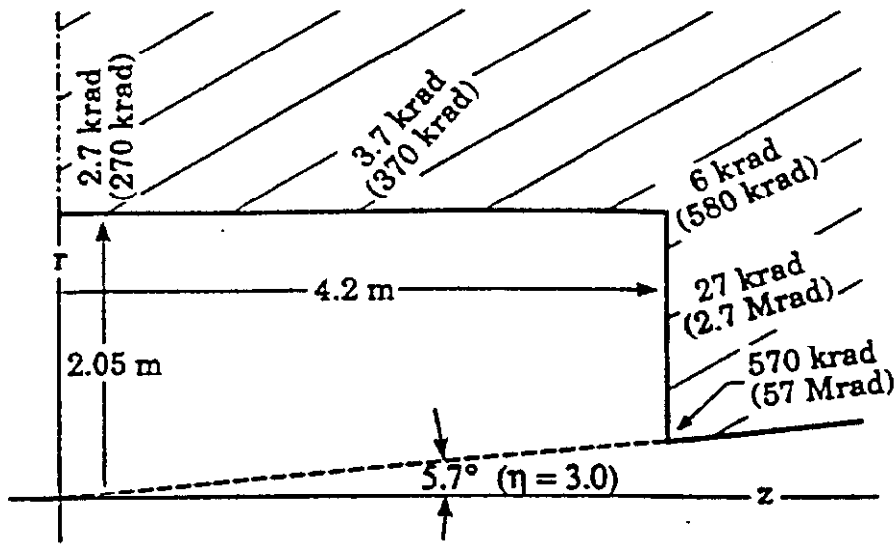


Fig. 2. The SDC radiation dose at EM shower maximum. The barrel region has a 100 year dose of <1 Mrad, while the endcap varies from 1 to 60 Mrad.

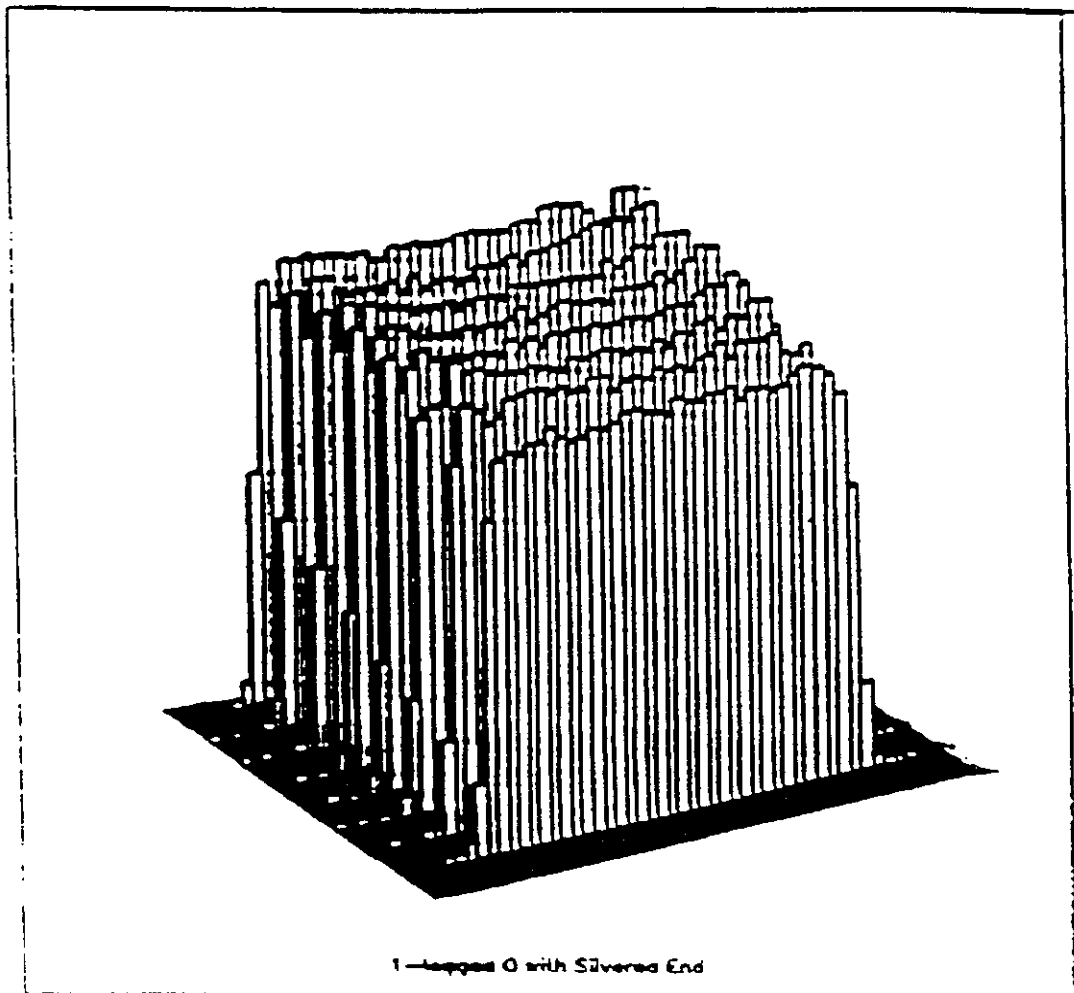
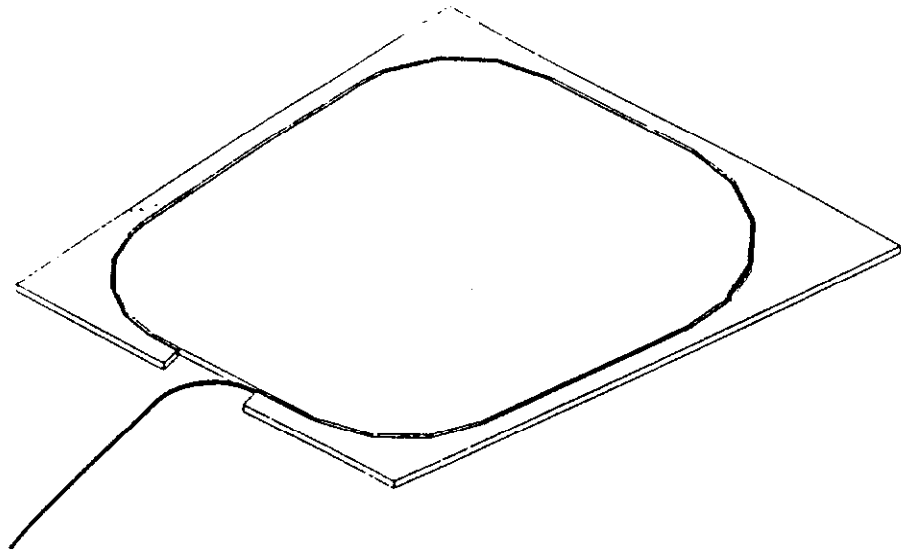


Fig. 3.a Layout of the tile/fiber optical system.

3.b Transverse scan of the tile/fiber response. The rms deviation from uniformity is 2%.

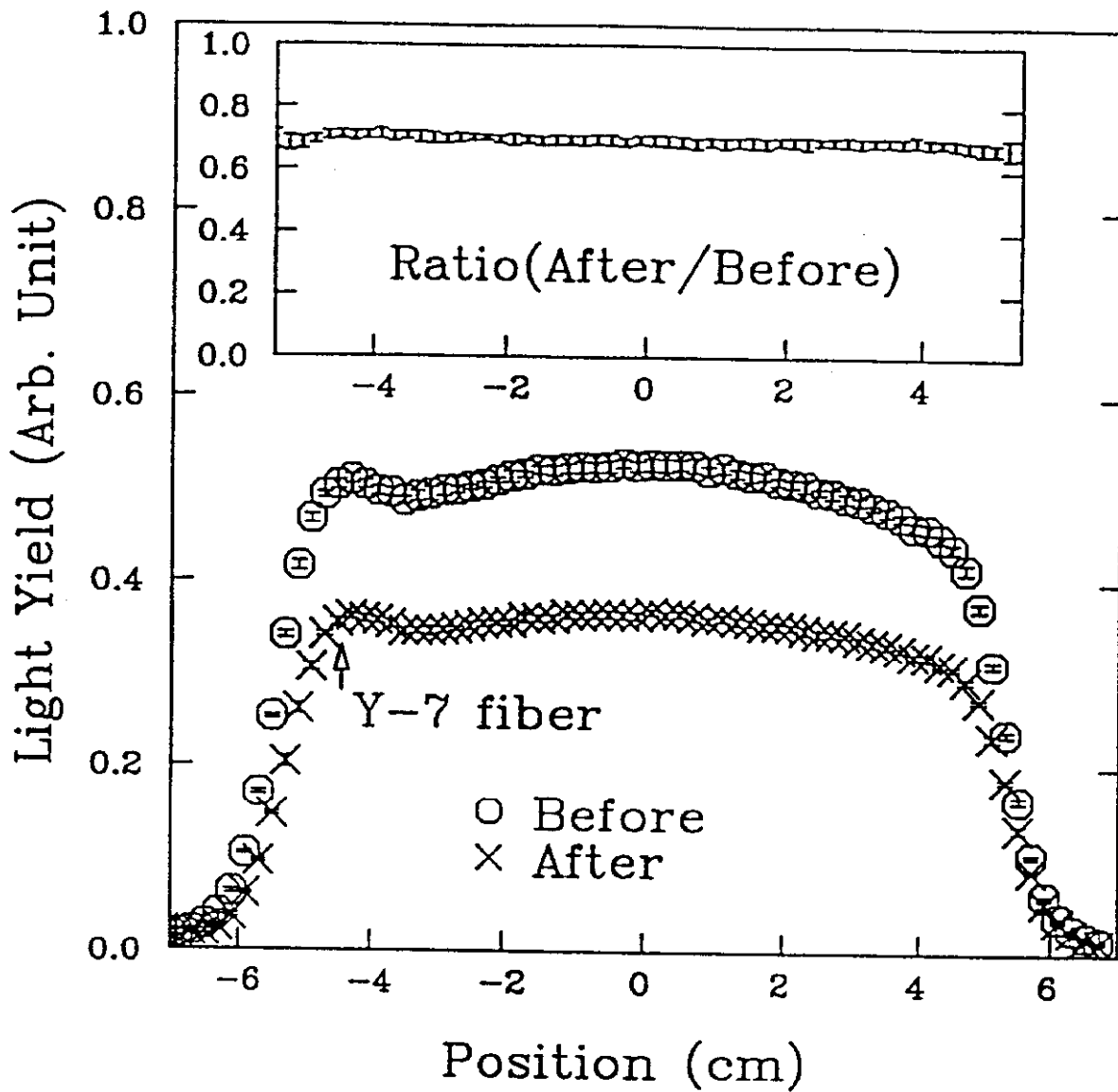


Fig. 4. Tsukuba data on transverse response before and after non-uniform irradiation.

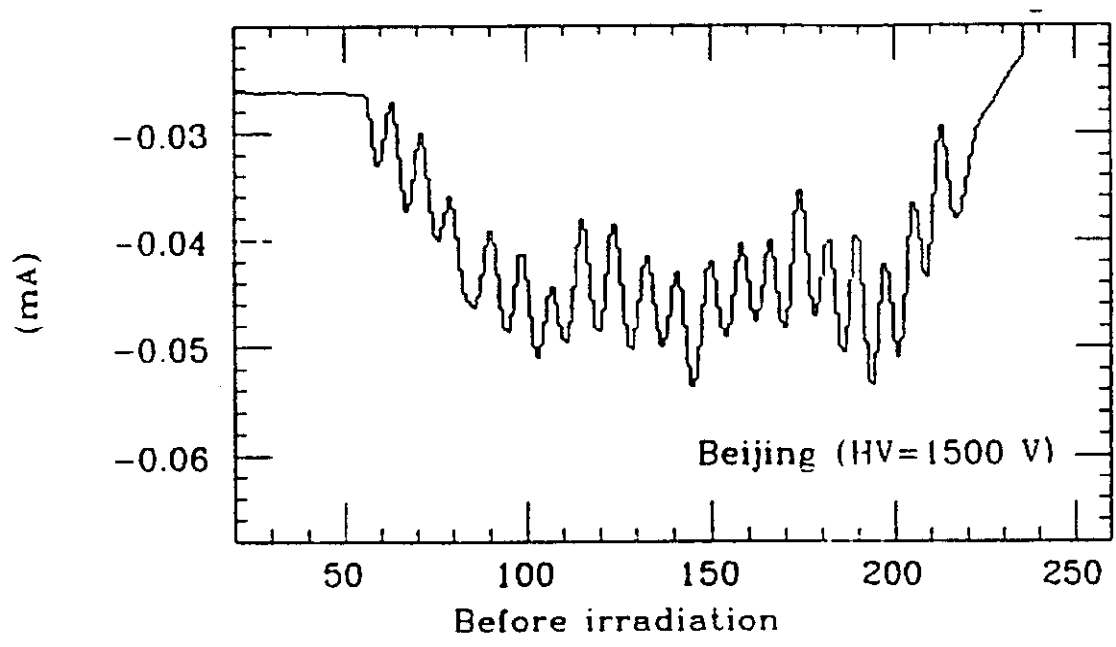
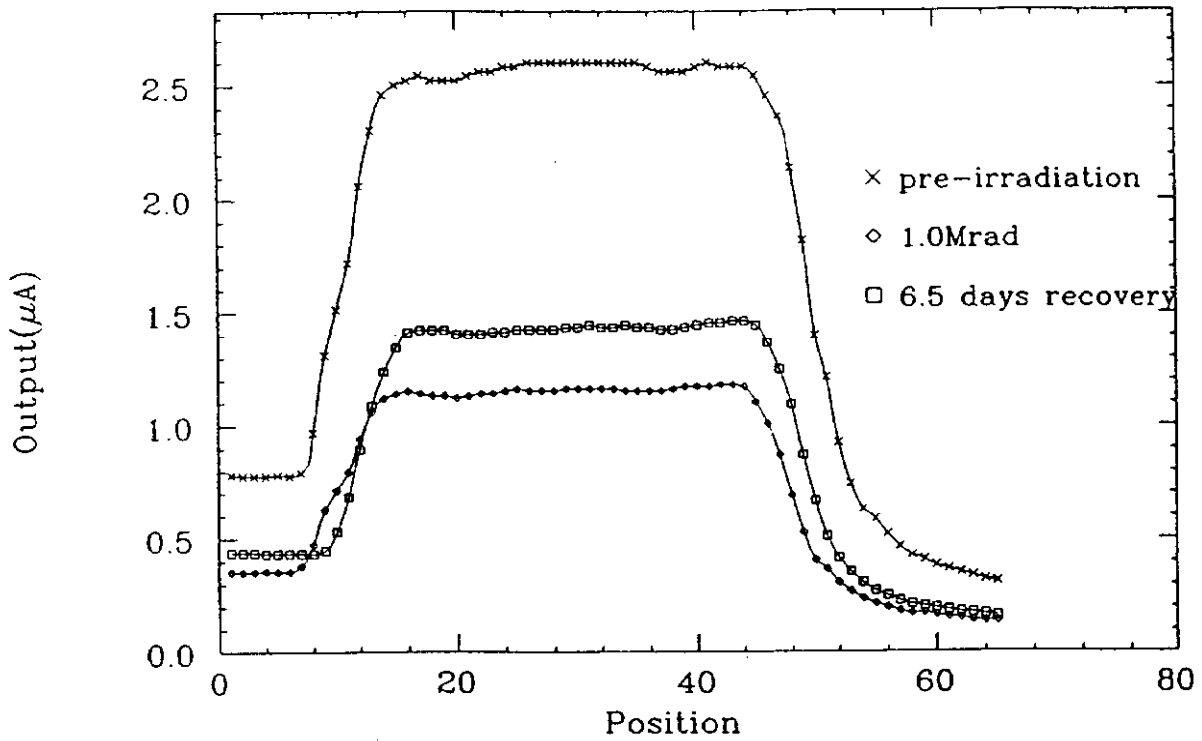


Fig. 5. Beijing data on longitudinal source scan before irradiation.

Module #3, T2



MODULE #3 L2 RECOVERY

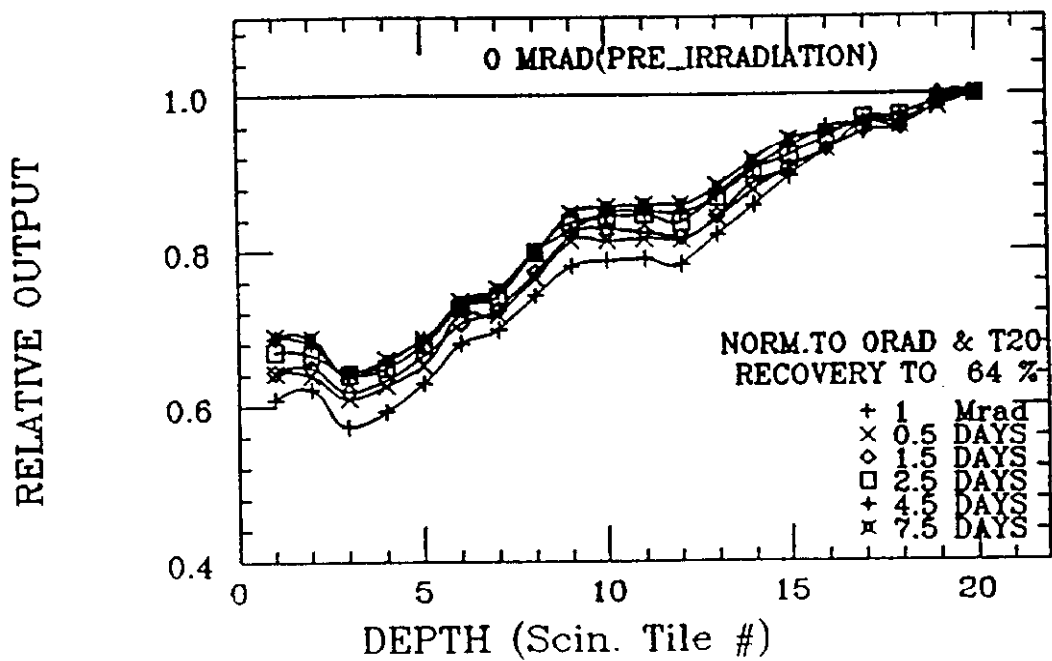


Fig. 6. Beijing data on transverse and longitudinal source scans for 1 Mrad irradiation and recovery.

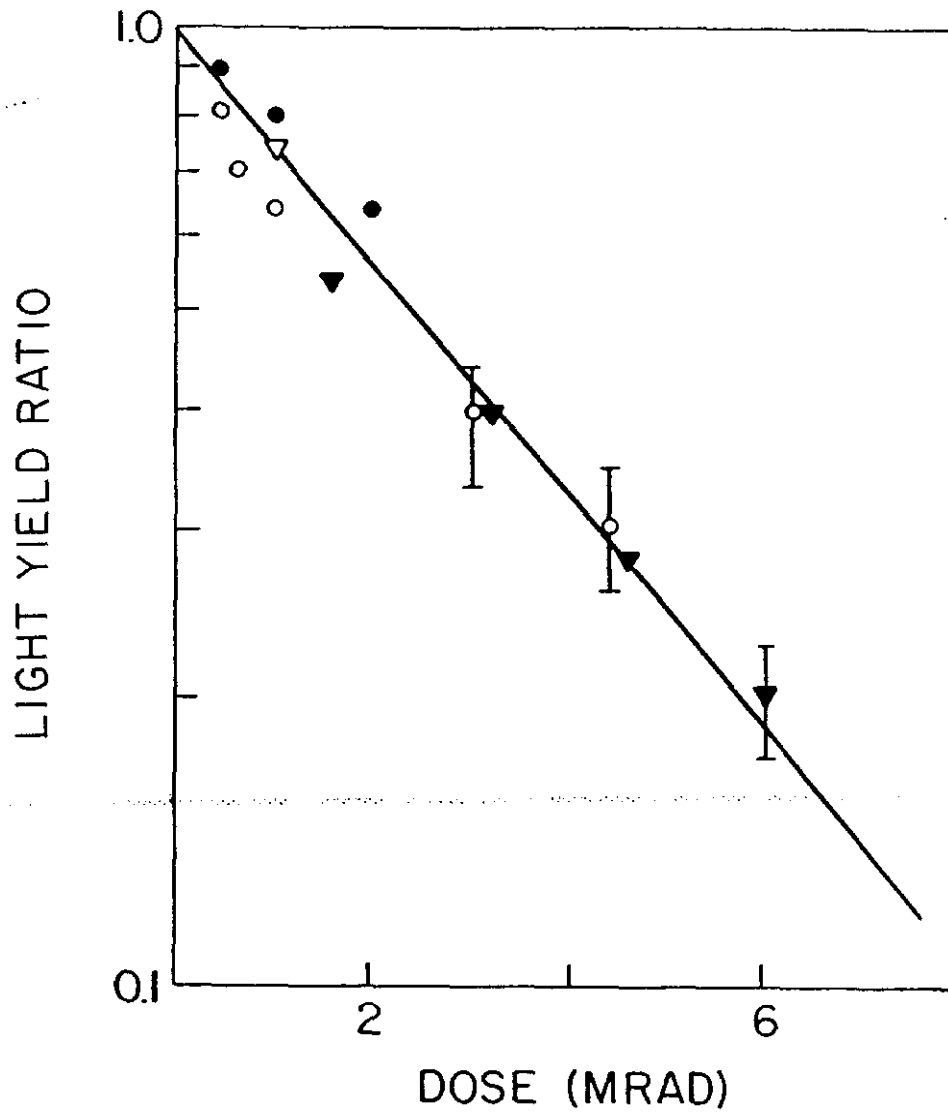


Fig. 7. Summary plot of light yield ratio at shower maximum for Saclay data •, o Tsukuba data, ▼ Beijing data. The line is of the form  $1 - [d(z)]_{\max} = \exp(-D / D_0)$ .

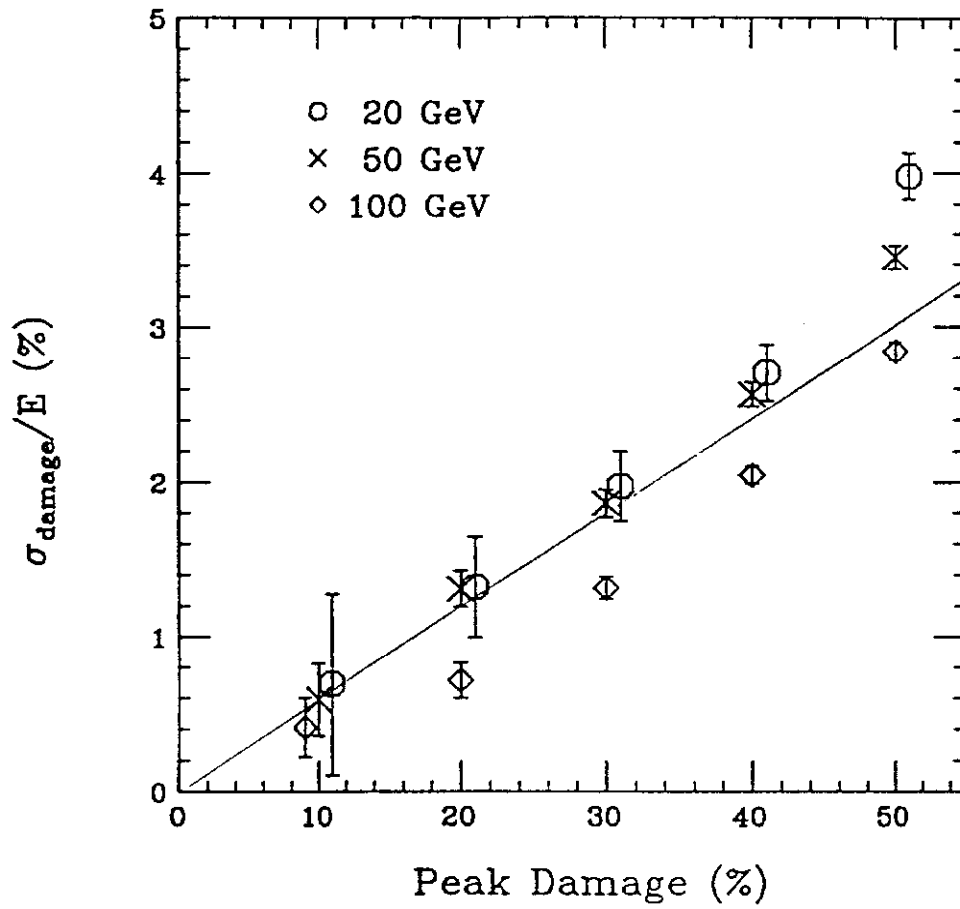


Fig. 8. Induced constant term in the fractional energy resolution as a function of the peak damage  $[d(z)]_{\text{max}}$  for different energies.

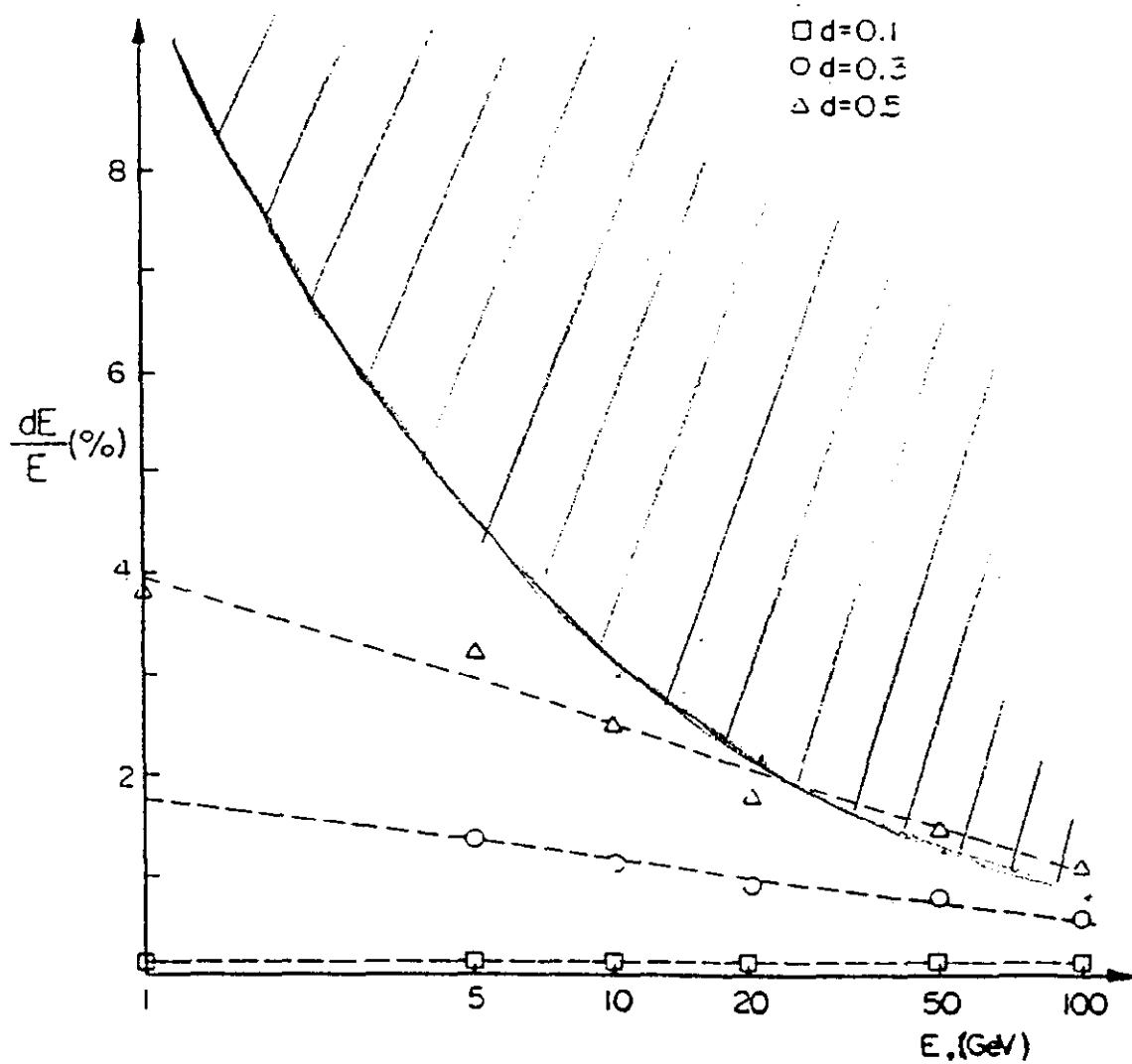


Fig. 9. Induced constant term in the fractional energy resolution as a function of energy for different peak damages,  $[d(z)]_{\max}$ . Simple corrections for conversion point fluctuations have been made using 2 longitudinal segments. The shaded region corresponds to errors greater than the assumed EM calorimeter resolution.

P = 15 GeV  
LAB E-DATA

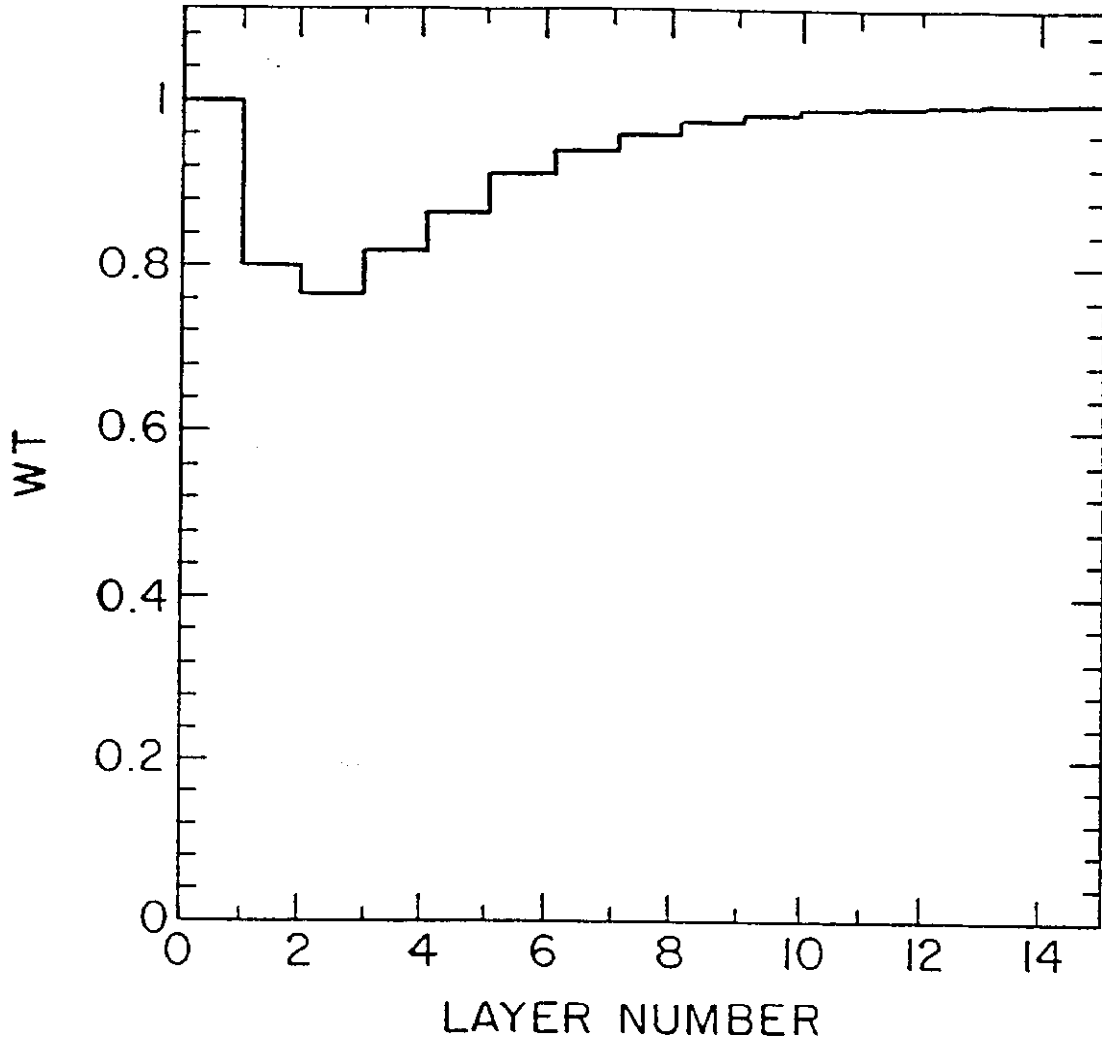


Fig. 10. Hadronic data at 15 GeV used to infer a hadronic response profile,  $WT(z) = 1 - d(z)$  assuming that damage is proportional to local energy deposition. A layer is 0.7 nuclear absorption lengths thick.

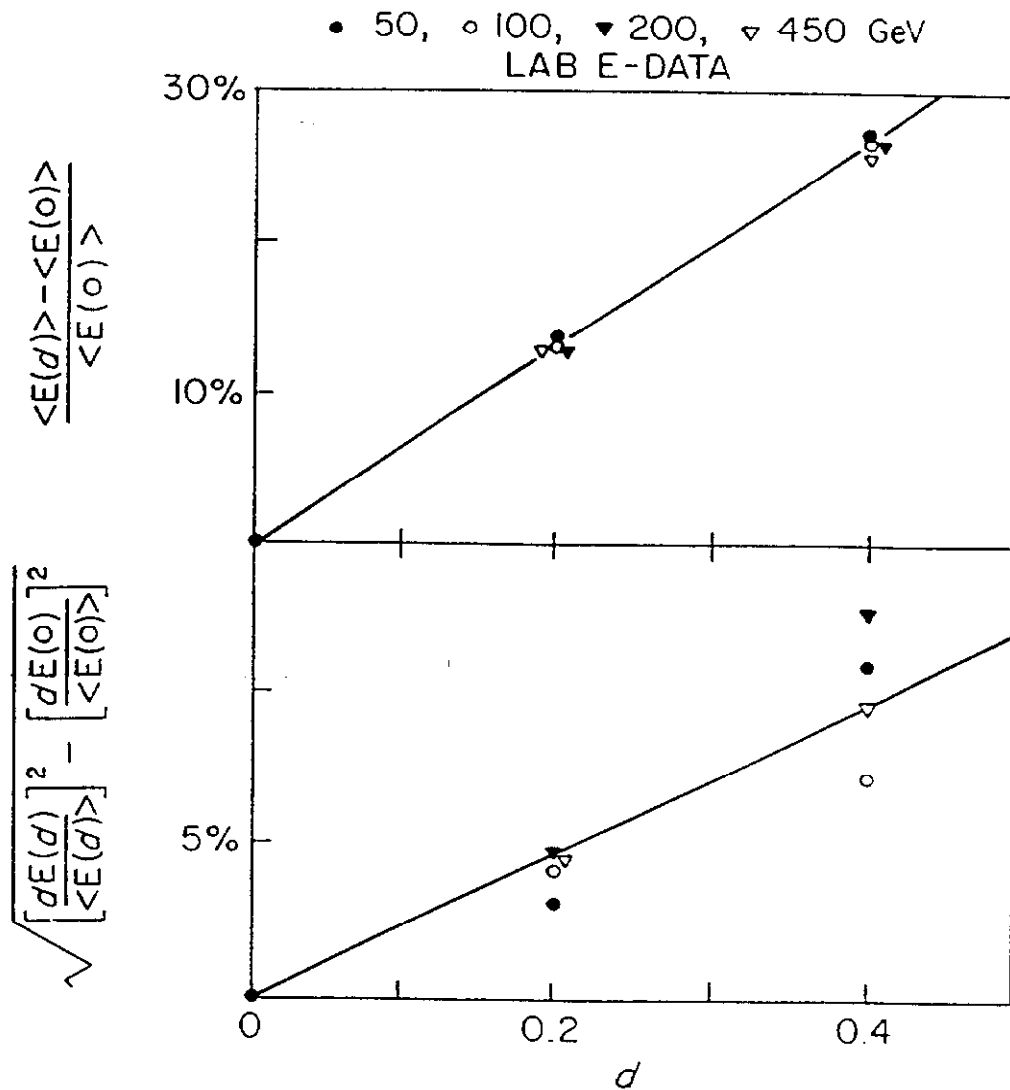


Fig. 11.a Mean induced nonlinearity as a function of peak hadronic damage for 4 different hadron energies

11.b Induced constant term in the fractional energy resolution as a function of the peak hadronic damage for 4 different hadron energies.